International Journal of Ocean System Engineering 1(2) (2011) 76-88
DOI 10.5574/IJOSE.2011.1.2.076

Hydroelastic Effects in Vibration of Plate and Ship Hull Structures Contacted with Fluid†

Jongsoo Lee[1] and Chang Yong Song[2*]

[1]*Department of Mechanical Engineering, Yonsei University, Seoul 120-749 Korea*

[2]*Department of Ocean Engineering, Mokpo National University, Jeonnam 534-729 Korea*

(Manuscript Received February 14, 2011; Revised March 30, 2011; Accepted May 2, 2011)

Abstract

The present study deals with the hydroelastic vibration analysis of structures in contact with fluid via coupled fluid-structure interaction (FSI) embedded with a finite element method (FEM) such that a structure displacement formulation is coupled with a fluid pressure–displacement formulation. For the preliminary study and validation of FEM based coupled FSI analysis, hydroelastic vibration characteristics of a rectangular plate in contact with fluid are first compared with the elastic vibration in terms of boundary condition and mode frequency. Numerical results from coupled FSI analysis have been shown to be rational and accurate, compared to energy method based theoretical solutions and experimental results. The effect of free surface on the vibration mode is numerically studied by changing the submerged depth of a rectangular plate. As a practical application, the hull structural vibration of 4,000 twenty–foot equivalent units (TEU) container ship is considered. Hydroelastic results of the ship hull structure are compared with those obtained from the elastic condition.

Keywords: Hydroelastic Vibration, Fluid-Structure Interaction (FSI), Coupled FSI Analysis, Submerged Depth, Container Ship

1. Introduction

The vibration of an elastic structure in contact with fluid has distinct features due to the effect of added mass, which is generated by the fluid pressure on the wetted surface of a submerged or floating structure such as a ship, an offshore structure, or a fluid tank. There are three kinds of significant vibration problems where the fluid-structure interaction (FSI) should be considered [1]. The first vibration problem is a relatively huge vibration that commonly occurs in elasto-acoustic problems such as the random flutter of an aircraft wing or the irregular motion of a suspension bridge. The second is a hydroelastic transient vibration caused by an underwater explosion or underwater impact loading. The third is a hydroelastic frequency-domain vibration of a submerged or floating structure due to FIS. For the study of the hydroelastic frequency-domain vibration of a structure in contact with fluid, a number of analytical methods have been developed to approximately evaluate the effect of the added mass using equivalent mapping function and model experiment [2–4]. Such methods facilitate the calculation of the added mass for the low frequency domain, and are computationally efficient. However, they can only be applied to a simple structure and are not be suitable for actual structures with complex shapes.

Finite element method (FEM) and/or boundary element method (BEM) based vibration analysis of a structure in contact with fluid has been practically applied to real-world applications. The coupled analysis employing FEM to both structure and fluid domains, or FEM to structure and BEM to fluid respectively has been widely used to solve vibration problems while considering the FSI phenomenon.

*Corresponding author. Tel.: +82-61-450-2732, Fax.: +82-61-452-7774.
E-mail address: cysong@mokpo.ac.kr.

Such method has been successfully validated not only from theoretical, numerical and experimental evaluations but also with some commercial FEM codes [5–8]. In the FEM-BEM based coupled analysis, the fluid–structure interaction effects are calculated in terms of generalized added masses using boundary integral equation and method of images. The FEM-BEM based coupled analysis is enhanced by the modal reanalysis scheme that is developed to solve the large coupled degrees of freedom based on from the Green function, and successfully applied to the vibration analysis of ships and offshore structures considering the FSI effects [9,10]. A hybrid method – a boundary integral equation method for FSI effects and FEM for structural analysis – is suggested to evaluate the effects of different end conditions on the dynamic response behavior of thin circular cylindrical shell structures in the full contact with internally flowing fluid [11]. In the FEM based coupled analysis, the effect of FSI is implemented by the added mass, which is generated by the potential of an idealized fluid satisfying the compatibility conditions on the interface in contact with fluid. An appropriate boundary condition is imposed on the free surface for the vibration analysis of partially filled or submerged, horizontal cylindrical shell [12]. Coupled hydroelastic vibration analysis and experiment have been conducted for the fluid-filled rectangular tank which is part of the equipment used in the ship hull structure [13]. An analytical method is developed to perform the coupled vibration analysis of the sloshing and bulging modes for a liquid-filled rigid circular cylindrical storage tank with an elastic annular plate in contact with sloshing surface of liquid [14]. A theoretical study on the free vibration characteristics of a number of perforated beams in contact with an ideal liquid is carried out by considering the compatibility conditions under FSI [15]. The FEM based vibration analysis and experiment are performed on a thin-walled hemi-ellipsoidal prolate dome under the elastic and external water-pressure conditions using FEM for both structure and fluid [16]. Modal and damping results of liquid sloshing container are evaluated for the surface tension and contact line boundary conditions using FEM [17].

The hydroelastic application of coupled analysis is especially significant in the context of the vibration of ship or offshore structures that have external contact with the infinite fluid domain. A 2D hydroelasticity theory has been successfully applied to a variety of beam-like merchant and naval ships in order to demonstrate its suitability to the symmetric, unsymmetric or anti-symmetric, and steady-state or dynamic behavior in waves [18]. The coupled analysis is theoretically applied to offshore structures using the full 3-D hydro-elasticity, where the Green function method is implemented in fluid domain and the finite element method is implemented in structure [19]. A comparison between coupled analysis theory and experimental measurements has been carried out for a fast patrol ship travelling in rough seas [20]. An idealized 2D/3D mono-hulled vessel treated as a flexible structure is adopted to predict and compare the dynamic characteristics using the FSI theory [21]. Dynamic behavior of bulk carrier hull structure is evaluated for both dry and wetted conditions, and the coupled analysis is applied to wet condition [22]. A ship structural vibration analysis procedure to estimate the global and local load effects considering symmetric and anti-symmetric hydroelastic conditions in high waves is proposed [23].

The present study explores the frequency-domain hydroelastic vibration of structures in contact with fluid via the coupled analysis embedded with a commercial FEM code, NASTRAN such that a structural displacement formulation is coupled with a fluid pressure–displacement formulation. The paper particularly focuses on investigating various hydroelastic effects on vibration analysios of structures in contact with fluid. The vibration analysis of a rectangular plate is first carried out to evaluate various hydroelastic effects on dynamic characteristics; this is a procedure for validating theoretical and experimental results. The practical application of coupled analysis is then presented for a container ship structural vibration. In the vibration analysis of rectangular plate, a number of parameters such as boundary condition, submerged depth, and vibratory mode are evaluated in respect of the hydroelastic vibration. The characteristics of hydroelastic vibration in contact with fluid are compared with the elastic results in dry condition.

Prior to the numerical analysis on the rectangular plate and ship hull structure, the basic theory is briefly reviewed in context of the FEM based coupled FSI analysis for hydroelastic vibration problem. In the numerical analysis of a rectangular plate, hydroelastic vibration characteristics are first

compared to the elastic vibration in terms of boundary condition and mode frequency. Vibration results from the coupled FSI analysis are compared and validated with energy method based theoretical solutions and experimental results [24]. The effect of submerged depth on the free surface is also discussed using results of hydroelastic vibration analysis. The coupled analysis is extended to a practical hydroelastic vibration analysis for the 4,000 twenty-foot equivalent units (TEU) container ship structure in contact with infinite sea water, and its results are compared with those of elastic vibration analysis in dry condition as well.

2. Fluid-Structure Interaction Theory [26]

In the FSI formulation, the governing equations for incompressible, inviscid, irrotational fluids are reconstructed into a matrix equation using the FEM where fluid pressures are the dependent variables while a matrix equation for the structure is typically formulated using the FEM. Mass and stiffness matrices are established based on a typical energy principle with the pressure taking the role of generalized displacement and the bounding surface displacement taking the role of the force function. The dynamics of the structure is described in the usual way with displacement taken as the dynamic variable and applied pressure taken as the force function. The linear dynamics is supposed for both the fluid and the structure in the formulation process, and the nodal matching compatibility is assumed at the wetted interface between the fluid and the structure. The free surface of fluid and the gravity constant are considered in the formulation while the surface tension is neglected [25-28].

2.1 Formulation of fluid domain

For an incompressible, inviscid, irrotational fluid with free surface, the complementary Euler-Lagrange matrix equation is defined as:

$$\begin{bmatrix} \bar{L}_{ff} & \bar{L}_{fw} & \bar{L}_{fi} \\ \bar{L}_{wf} & \bar{L}_{ww} & \bar{L}_{wi} \\ \bar{L}_{if} & \bar{L}_{iw} & \bar{L}_{ii} \end{bmatrix} \begin{Bmatrix} p_f \\ p_w \\ p_i \end{Bmatrix} = \begin{Bmatrix} P_f \\ P_w \\ 0 \end{Bmatrix} \tag{1}$$

where, $\bar{L}$, p and P are the fluid interface matrix, the pressure and the generalized force imparted to the fluid, respectively. The pressure partitions p_f, p_w and p_i correspond to the free surface, the wetted interface and the internal fluid pressure sets, respectively. The generalized force on the fluid interior is zero from the assumption of the uniform gravity. In the formulation of fluid domain, pressure variables are defined at undisturbed positions in space. As a free surface is displaced, the free surface pressure p_f is defined in terms of the outward normal displacement of the fluid free surface u_f as follows:

$$p_f = \rho g u_f \tag{2}$$

where, ρ and g are fluid density and gravity constant, respectively. By multiplying Eqn. (2) by the free surface area matrix A_{ff} , which is a symmetric positive definite matrix, the equation becomes:

$$K_{ff} u_f - A_{ff} p_f = 0 \tag{3}$$

where, the free surface stiffness matrix K_{ff} is given by:

$$K_{ff} \equiv \rho g A_{ff} \tag{4}$$

The inverse form of the free surface stiffness matrix K_{ff} can be present by considering the symmetric positive definite maxtrix. Multiplying Eqn. (3) by $A_{ff}^T K_{ff}^{-1}$ and twice the differentiation with respect to time yields:

$$A_{ff}^T \ddot{u}_f - M_{ff} \ddot{p}_f = 0 \tag{5}$$

where, the free surface mass matrix M_{ff} is defined as follows:

$$M_{ff} \equiv A_{ff}^T K_{ff}^{-1} A_{ff} \ . \tag{6}$$

This matrix is also symmetric positive definite. The double dot denotes twice the differentiation with respect to time, and T denotes the transpose of a matrix. The fluid free surface mass matrix is used in calculating the slosh modes of the fluid in a rigid structure. The generalized force in the fluid at the free surface is related to the outward normal displacement through the free surface area matrix and the flow relationship as follows:

$$p_f = -A_{ff}^T \ddot{u}_f \ . \tag{7}$$

Static condensation of the interior pressure p_i from Eqn. (1) as well as incorporating Eqns. (5) and (7) becomes:

$$\begin{bmatrix} M_{ff} & 0 \\ 0 & 0 \end{bmatrix} \begin{Bmatrix} \ddot{p}_f \\ \ddot{p}_w \end{Bmatrix} + \begin{bmatrix} L_{ff} & L_{fw} \\ L_{wf} & L_{ww} \end{bmatrix} \begin{Bmatrix} p_f \\ p_w \end{Bmatrix} = \begin{Bmatrix} 0 \\ p_w \end{Bmatrix} \tag{8}$$

Eqn.(8) is the general symmetric matrix equations of a fluid; this equation is now applied to the coupled FSI formulation for solving the hydroelastic vibration problem.

2.2 Formulation of structure domain

In a structure domain, the matrix equation of vibration problem is generally defined as follows:

$$\begin{bmatrix} M_{bb} & M_{bc} \\ M_{cb} & M_{cc} \end{bmatrix} \begin{Bmatrix} \ddot{u}_b \\ \ddot{u}_c \end{Bmatrix} + \begin{bmatrix} K_{bb} & K_{bc} \\ K_{cb} & K_{cc} \end{bmatrix} \begin{Bmatrix} u_b \\ u_c \end{Bmatrix} = \begin{Bmatrix} F_b \\ F_c \end{Bmatrix} \tag{9}$$

where, M and K are the mass and stiffness matrices, respectively, F the excited forces, and u_b and u_c the structural displacement sets corresponding to the fluid interface displacements and the remainder of the displacements, respectively. In Eqn. (9), the damping matrix is not included in the formulation.

2.3 Formulation of Coupled FSI

The generalized fluid force at the wetted interface is related to the structure displacement through the wetted surface area matrix and the flow relationship, and is defined similarly to Eqn. (7) as follows:

$$p_w = -A_{bw}^T \ddot{u}_b \tag{10}$$

where, A_{bw} is the wetted surface area matrix. The fluid applies forces over the structure surface area as follows:

$$F_b = A_{bw} p_w - K_g u_b \tag{11}$$

where, K_g is the gravity stiffness matrix. For most engineering applications, K_g is much smaller than structure stiffness K_{bb} in Eqn. (9), and is able to be neglected in the coupled FSI formulation. The combination of the fluid and structure Eqns. (8) and (9) into a matrix equation incorporating Eqns. (10) and (11) yields:

$$\begin{bmatrix} M_{ff} & 0 & 0 & 0 \\ 0 & 0 & A_{bw}^T & 0 \\ 0 & 0 & M_{bb} & M_{bc} \\ 0 & 0 & M_{cb} & M_{cc} \end{bmatrix} \begin{Bmatrix} \ddot{p}_f \\ \ddot{p}_w \\ \ddot{u}_b \\ \ddot{u}_c \end{Bmatrix} + \begin{bmatrix} L_{ff} & L_{fw} & 0 & 0 \\ L_{wf} & L_{ww} & 0 & 0 \\ 0 & -A_{bw} & K_{bb} & K_{bc} \\ 0 & 0 & K_{cb} & K_{cc} \end{bmatrix} \begin{Bmatrix} p_f \\ p_w \\ u_b \\ u_c \end{Bmatrix} = \begin{Bmatrix} 0 \\ 0 \\ 0 \\ F_c \end{Bmatrix} \tag{12}$$

Eqn. (12) is the non-symmetric coupled fluid-structure formulation. Solving the second row in Eqn. (12) for p_w, substituting back into the matrix equation yields:

$$\begin{bmatrix} M_{ff} & -A_{bf}^T & 0 \\ 0 & M_{bb} + m_{bb} & M_{bc} \\ 0 & M_{cb} & M_{cc} \end{bmatrix} \begin{Bmatrix} \ddot{p}_f \\ \ddot{u}_b \\ \ddot{u}_c \end{Bmatrix} + \begin{bmatrix} \widetilde{L}_{ff} & 0 & 0 \\ A_{bf} & K_{bb} & K_{bc} \\ 0 & K_{cb} & K_{cc} \end{bmatrix} \begin{Bmatrix} p_f \\ u_b \\ u_c \end{Bmatrix} = \begin{Bmatrix} 0 \\ 0 \\ F_c \end{Bmatrix} \tag{13}$$

where,

$$m_{bb} \equiv A_{bw} L_{ww}^{-1} A_{bw}^T \tag{14}$$

$$\widetilde{L}_{ff} \equiv L_{ff} - L_{fw} L_{ww}^{-1} L_{wf} \tag{15}$$

$$A_{bf} \equiv A_{bw} L_{ww}^{-1} L_{wf} \tag{16}$$

The matrix m_{bb} is usually called the added mass of the fluid to the structure. Eqn. (13) is still non-symmetric, but can be transformed into a symmetric form through a series of transformations. The key step in the transformations is to use the slosh modes. Solving the eigenvalue problem for the first row in Eqn. (13) after inserting $\{\ddot{u}_b\} = 0$ (rigid container), the modified equation is defined as follows:

$$M_{ff} \ddot{p}_f + \widetilde{L}_{ff} p_f = 0 \tag{17}$$

The slosh modes ϕ_{ff} are obtained with respect to Eqn. (17) as follows:

$$p_f \equiv \phi_{ff} q_f \tag{18}$$

$$I_{ff} \equiv \phi_{ff}^T M_{ff} \phi_{ff} \tag{19}$$

$$W_{ff} \equiv \phi_{ff}^T \widetilde{L}_{ff} \phi_{ff} \tag{20}$$

where, q_f is a vector of generalized coordinates, I_{ff} is an identity matrix, and W_{ff} is a diagonal matrix with the circular frequency squared on the diagonal. All slosh modes are retained; no modal truncation is used in the eigensolution. Using the slosh modes, Eqn. (13) can be converted into the following form:

$$\begin{bmatrix} I_{ff} & -\phi_{ff}^T A_{bf}^T & 0 \\ 0 & M_{bb} + m_{bb} & M_{bc} \\ 0 & M_{cb} & M_{cc} \end{bmatrix} \begin{Bmatrix} \ddot{q}_f \\ \ddot{u}_b \\ \ddot{u}_c \end{Bmatrix} + \begin{bmatrix} W_{ff} & 0 & 0 \\ A_{bf} \phi_{ff} & K_{bb} & K_{bc} \\ 0 & K_{cb} & K_{cc} \end{bmatrix} \begin{Bmatrix} q_f \\ u_b \\ u_c \end{Bmatrix} = \begin{Bmatrix} 0 \\ 0 \\ F_c \end{Bmatrix} \tag{21}$$

The matrix $\widetilde{L}_{ff}$ has a rank deficiency of one because the incompressible fluid volume does not change under the static uniform pressure. A well-known theorem in linear algebra states that for a symmetric matrix A, the equation $Ax = 0$ has a nontrivial solution $x \neq 0$ if and only if determi-

nant $A = 0$. Hence, $\widetilde{L}_{ff}$ is singular, and a rigid body slosh mode exists in which its frequency is nearly zero. Partitioning the generalized coordinates q_f into q_r corresponding to the zero frequency slosh mode and q_n corresponding to the rest of slosh modes, the diagonal matrix is defined as follows:

$$W_{ff} = \begin{bmatrix} W_{rr} & 0 \\ 0 & W_{nn} \end{bmatrix} \tag{22}$$

Applying the condition $W_{rr} = 0$ to Eqn. (21)

$$\begin{bmatrix} I_{rr} & 0 & -A_{br}^T & 0 \\ 0 & I_{nn} & -A_{bn}^T & 0 \\ 0 & 0 & M_{bb}+m_{bb} & M_{bc} \\ 0 & 0 & M_{cb} & M_{cc} \end{bmatrix} \begin{Bmatrix} \ddot{q}_r \\ \ddot{q}_n \\ \ddot{u}_b \\ \ddot{u}_c \end{Bmatrix} + \begin{bmatrix} 0 & 0 & 0 & 0 \\ 0 & W_{nn} & 0 & 0 \\ A_{br} & A_{bn} & K_{bb} & K_{bc} \\ 0 & 0 & K_{cb} & K_{cc} \end{bmatrix} \begin{Bmatrix} q_r \\ q_n \\ u_b \\ u_c \end{Bmatrix} = \begin{Bmatrix} 0 \\ 0 \\ 0 \\ F_c \end{Bmatrix} \tag{23}$$

where, $A_{bf}\phi_{ff} \equiv \begin{bmatrix} A_{br} & A_{bn} \end{bmatrix}$ and $I_{rr} = 1$. The term A_{br} represents the shape taken by the wetted part of the container in order to yield the rigid body slosh mode. It means that the free surface of the fluid rises uniformly as the container is statically squeezed into this shape. From the first row of Eqn. (23), the generalized coordinate corresponding to the rigid body slosh mode is obtained in terms of the wetted structure displacement as follows:

$$q_r = I_{rr}^{-1} A_{br}^T u_b \tag{24}$$

By substituting Eqn. (24) into Eqn. (23), the reduced form of Eqn. (23) is defined as follow:

$$\begin{bmatrix} I_{nn} & -A_{bn}^T & 0 \\ 0 & M_{bb}+m_{bb} & M_{bc} \\ 0 & M_{cb} & M_{cc} \end{bmatrix} \begin{Bmatrix} \ddot{q}_n \\ \ddot{u}_b \\ \ddot{u}_c \end{Bmatrix} + \begin{bmatrix} W_{nn} & 0 & 0 \\ A_{bn} & K_{bb}+k_{bb} & K_{bc} \\ 0 & K_{cb} & K_{cc} \end{bmatrix} \begin{Bmatrix} q_n \\ u_b \\ u_c \end{Bmatrix} = \begin{Bmatrix} 0 \\ 0 \\ F_c \end{Bmatrix} \tag{25}$$

where,

$$k_{bb} = A_{br} I_{rr}^{-1} A_{br}^T \tag{26}$$

The matrix W_{nn} is a symmetric positive definite matrix, and hence its inverse exists. By multiplying the first row of Eqn. (25) by $-A_{bn}W_{nn}^{-1}$, adding the resulting equation to the second row, and multiplying the first row by W_{nn}^{-1}, the final form of the coupled fluid-structure equation is obtained as follows:

$$\begin{bmatrix} W_{nn}^{-1} & -W_{nn}^{-1}A_{bn}^T & 0 \\ -A_{bn}^T W_{nn}^{-1} & M_{bb}+m_{bb}+\mu_{bb} & M_{bc} \\ 0 & M_{cb} & M_{cc} \end{bmatrix} \begin{Bmatrix} \ddot{q}_n \\ \ddot{u}_b \\ \ddot{u}_c \end{Bmatrix} + \begin{bmatrix} I_{nn} & 0 & 0 \\ A_{bn} & K_{bb}+k_{bb} & K_{bc} \\ 0 & K_{cb} & K_{cc} \end{bmatrix} \begin{Bmatrix} q_n \\ u_b \\ u_c \end{Bmatrix} = \begin{Bmatrix} 0 \\ 0 \\ F_c \end{Bmatrix} \tag{27}$$

where,

$$\mu_{bb} \equiv A_{bn} W_{nn}^{-1} A_{bn}^T \tag{28}$$

Eqn. (27) is now symmetric, and no approximation is used in the series of transformations in order to lead to this equation from the original non-symmetric Eqn. (12). Such symmetric form is possible to solve the coupled FSI vibration problems.

3. Vibration of Rectangular Plate

Prior to conducting the coupled analysis into a practical structure, the validation of the proposed analysis is applied for a rectangular plate since boundary conditions are definitely realized in experimental and analytical solutions. That is, such simplified structure is expediently used to evaluate various hydroelastic effects on vibration analysis, which is compared with the analytical solution and experimental result. The hydroelastic vibration characteristics are to be compared with the elastic results in terms of boundary condition, order of vibratory mode and submerged depth from free surface. A commercial finite element software, NASTRAN [25] is used for both elastic and hydroelastic vibration analyses of which the detailed procedures are depicted in Figure 1. The major dimensions and material properties of the rectangular plate are summarized in Table 1. For the hydroelastic vibration analysis, the submerged depth from the free surface and the fluid type are presented in Figure 2. The finite element model of the rectangular plate is generated using the SHELL element (type) as shown in Figure 3. A total of 900 elements and 961 nodes are used in the finite element model. The wetted surface is defined such that plate elements are in contact with the fluid; all of plate elements have the interface with fluid at both top and bottom sides as shown in Figure 2.

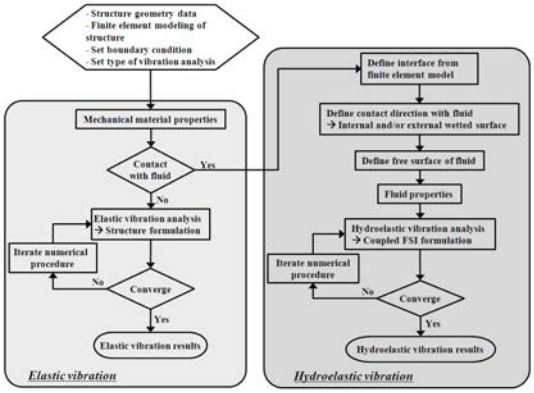

Fig. 1. Elastic and hydroelastic vibration analysis procedure

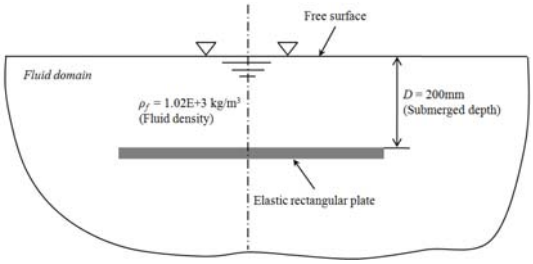

Fig. 2. Rectangular plate submerged in fluid

Table 1. Steady-state error (%)

Property	Young's modulus (N/m^2)	Poisson's ratio	Density (kg/m^3)
Value	1.961E+11	0.30	7.85E+3
Dimension	Width × Height × Thickness = 600mm × 600mm × 3.2mm		

For the validation of FEM solutions, the solutions are compared with the energy method based theoretical results and experimental data [24]. The energy method based analytical formulation for the plate vibration is defined as follows [29]:

$$\omega_{ij} = \frac{\lambda_{ij}^2}{2\pi ab}\left[\frac{Eh^3}{12\gamma(1-\nu^2)}\right]^{1/2}, \quad (23)$$

$$\lambda_{ij}^2 = \pi^2\left[i^2 + j^2\left(\frac{a}{b}\right)^2\right], \quad (24)$$

$$\gamma = \rho_S h . \quad (25)$$

In above expressions, ω is the normal mode frequency, λ is a coefficient of the vibration mode, a and b are width and height of the plate, respectively, h is the plate thickness, E is Young's modulus of the plate, γ is the mass per unit area, and v is Poisson's ratio. In Eqns. (24) and (25), i and j denote mode sequences, and ρ_S is the density of the plate. The analytical solution of the plate in contact with fluid is analogous to the following equation:

$$\omega_{hydro-elastic} = \omega_{elastic}\frac{1}{\sqrt{1+\varepsilon}} \quad (26)$$

where, ε is the parameter for the added mass and defined as follows:

$$\varepsilon = \alpha \cdot \frac{\rho_F}{\rho_S} \cdot \frac{a}{h} \quad (27)$$

where,

$$\alpha = \frac{2}{\pi} \cdot \frac{1}{\sqrt{1+\left(\frac{a}{b}\right)^2}} \quad (28)$$

In Eqn. (27), α is a coefficient for the condition of a surrounding fluid and ρ_F represents the density of fluid. The experiment has been carried out with respect to boundary condition and order of vibratory mode. The hydroelastic vibration experiment is performed in a model cistern – 6.0 m (length) × 2.0 m (breadth) × 1.5 m (depth) in size – considering the effect of the submerged depth in fluid. The vibration frequencies and mode shapes are measured using exciter, accelerometer, analyzer, etc. The experiment in a model cistern containing fluid is also repeated in dry conditions [24].

A number of boundary conditions on the rectangular plate are selected to identify the hydroelastic vibration characteristics as shown in Figure 3. For the various boundary conditions, the results of coupled analysis are compared with both the energy method based analytical solutions and experimental ones as summarized in Table 2. Hydroelastic vibration analyses of the first normal mode are carried out for all types of boundary conditions. The results of frequency and mode shape are compared with the elastic vibration analysis in dry condition to see the fluid effects on the vibration of rectangular plate as shown in Table 2 and Figure 4, wherein the mode frequency and the magnitude of mode shape are decreased in fluid compared to the results in dry condition.

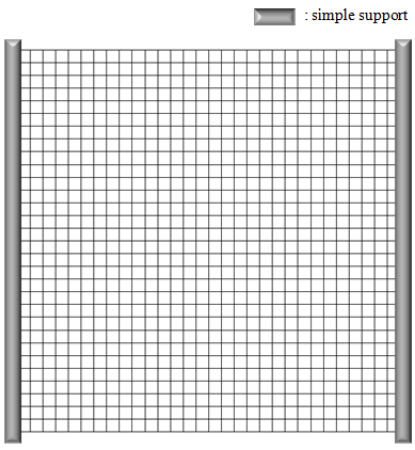

(a) Simple-simple and free-free [S-S, F-F] boundary condition

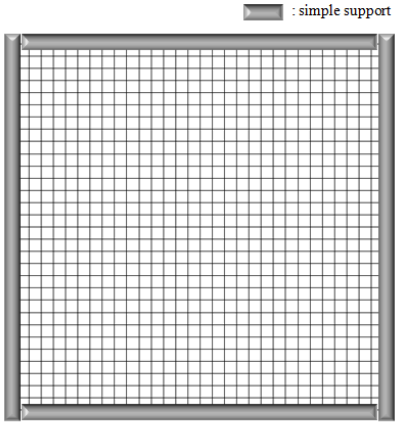

(b) Simple-simple and simple-simple [S-S, S-S] boundary condition

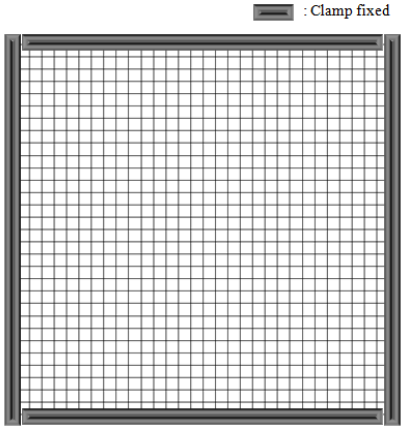

(c) Clamp-clamp and clamp-clamp [C-C, C-C] boundary condition

Fig. 3. Finite element model and boundary conditions for rectangular plate

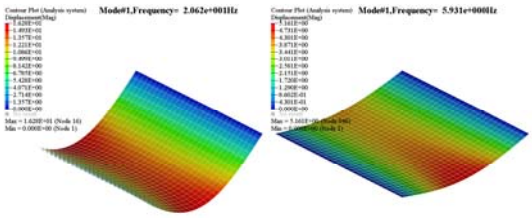

a) S-S, F-F boundary condition (left: elastic, right: hydroelastic)

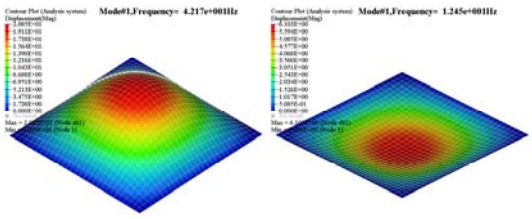

(b) S-S, S-S boundary condition (left: elastic, right: hydroelastic)

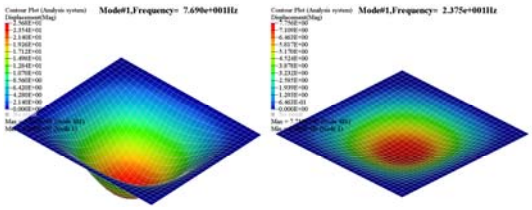

(c) C-C, C-C boundary condition (left: elastic, right: hydroelastic)

Fig. 4. Elastic and hydroelastic vibration mode shapes for various boundary conditions

Table 2. The first normal mode frequency of rectangular plate according to boundary condition [unit: Hz]

	Boundary condition	FEM (Coupled analysis)	Analytical solution (Energy method)	Experiment
Elastic	S-S, F-F	20.62	20.60	20.80
	S-S, S-S	42.17	42.20	40.00
	C-C, C-C	76.90	78.00	72.00
Hydroelastic	S-S, F-F	5.93	6.20	5.40
	S-S, S-S	12.45	12.70	10.60
	C-C, C-C	23.75	23.40	20.00

The decrement is found for all types of boundary conditions since the added mass as defined Eqn. (22) seems to be affected on the structure-fluid interface. The decrement ratio of hydroelastic vibration frequency is remarkable in case of the simple-simple and free-free (S-S, F-F) boundary condition comparing to the clamp-clamp and clamp-clamp

(C-C, C-C) condition. A mass effect on the hydroelastic motion increases as the boundary condition becomes reduced. Thus, the fluid effect on the vibration of structure in contact with fluid should be significantly considered in a floating structure. It is also proved that FEM based results are rational compared to analytical solutions and experimental results for both in dry and wetted conditions as represented in Table 2. The fluid effect on vibration mode order is reviewed as the mode is increased up to the fourth order. The simple-simple and simple-simple (S-S, S-S) boundary condition is adopted for the evaluation of mode effect. The frequencies of four mode shapes are obtained from FEM based analysis, theoretical formulation and experiment, and are demonstrated in Table 3 and Figures 5 to 6.

Table 3. Mode effect on hydroelastic vibration of rectangular plate in contact with fluid [unit: Hz]

Mode sequence	FEM (Coupled analysis)	Analytical solution (Energy method)	Experiment
1-1	12.45	12.70	10.60
1-2	39.44	31.68	33.00
2-2	71.82	50.69	65.00
1-3	94.07	63.37	85.00

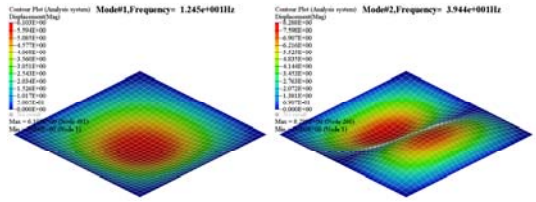

(a) 1-1(left) and 1-2(right) modes

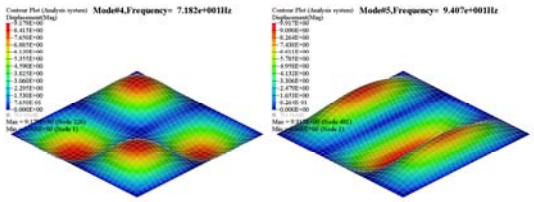

(b) 2-2(left) and 1-3(right) modes

Fig. 5. Hydroelastic vibration mode shapes according to order increment

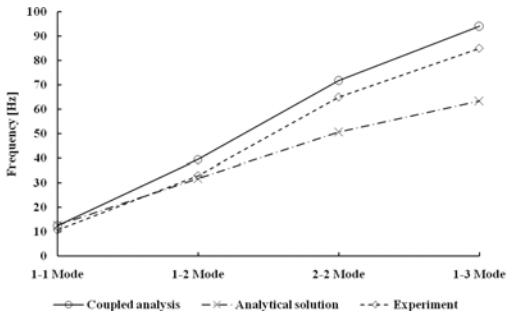

Fig. 6. Comparison of mode effect on hydroelastic vibration of rectangular plate in contact with fluid

In these results, the FEM based coupled analysis results tend to be more consistent with experimental results than analytical solutions as the mode sequence is increased. The vibration mode in energy method is calculated based on considering the structural geometry values of a and b as defined in Eqn. (24) while the coupled analysis includes both mass and stiffness terms for complete vibration modes as represented in Eqn. (27). Therefore, the coupled analysis is appropriate for evaluating the high mode vibration of structure in contact with fluid. The effect of the submerged depth from free surface is evaluated using the coupled analysis. The wetted surface is defined only at the bottom side for the analysis cases of the submerged depth of 0.1 mm and t/2 mm – half of thickness of rectangular plate, while others have an interface with fluid at both top and bottom sides, covering the full submergence. The submerged depth effect is explored for simple-simple and free-free (S-S, F-F) boundary condition which represents the prominent hydroelastic effect as mentioned above. The first mode frequencies are evaluated according the variation of the submerged depth as represented in Table 4 and Figure 7.

Table 4. Submerged depth effect on hydroelastic vibration of rectangular plate in contact with fluid

Submerged depth [mm]	0.1	t/2	50	100	150	200	250	∞
Frequency [Hz] (Coupled analysis)	20.6	6.88	6.39	6.15	6.01	5.93	5.88	5.81

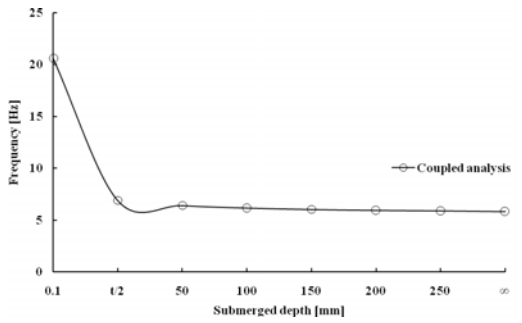

Fig. 7. Submerged depth effect on hydroelastic vibration of rectangular plate in contact with fluid

These results show that the hydroelastic effect on vibration is remarkably increased as half of thickness of rectangular plate is submerged in fluid. After the plate is fully sunk in fluid, the submerged depth has little effect on vibration characteristics up to an infinite depth because fluid boundary condition is considered only on the fluid-structure interface in the coupled analysis.

4. Vibration of Ship Hull Structure

Both elastic and hydroelastic vibration characteristics of an actual ship structure are now explored to emphasize the significance of the hydroelastic effect on a practical application using a commercial code, NASTRAN. The main characteristics of container ship are represented in Table 5. In Table 5, RPM, BHP, MCR and NCR denote revolutions per minute, brake horsepower, maximum continuous rating, and normal continuous rating, respectively.

Table 5. Main characteristics of container ship

	Property	Value
Ship particulars	Type	4,000 TEU container carrier
	Length	245.0 m
	Breadth	32.2 m
	Depth	19.0 m
	Ship speed	23.8 knots
Main engine particulars	Type	2 Strokes
	Bore / Stroke	900 mm / 3,188 mm
	# of cylinders	8
	Power at MCR	49,680 BHP at 104 RPM
	Power at NCR	44,710 BHP at 100.4 RPM
Propeller particulars	Type	Fixed pitch propeller
	# of blades	5

Ship vibratory responses are mainly caused by the excitation forces from the main engine and propeller propulsion. The main excitation frequencies due to main engine and propeller are summarized in Table 6. In a case where such results are applied to the vibration based design, modal frequencies of ship hull structure should not be resonant with main excitation frequencies under the operating range from NCR to MCR. The ship hull structure of container carrier has large openings on the deck level to load a number of containers. This type of a ship structure has relatively low torsion stiffness in terms of large openings. In the vibration analysis of container ship, complex modes appear to the vertical mode, the coupled torsion–horizontal mode and local modes since the opening of structure generally results in a large difference between centroid and shear center [30].

Table 6. Main excitation frequencies

[unit: Hz]

Excitation Sources	Order	NCR	MCR	Remarks
Main engine	8th	13.387	13.867	# of cylinders: 8
Propeller	1st	8.367	8.667	# of blades: 5

The FE model of a ship hull structure is shown in Figure 8(a), wherein the half breadth of a ship is used to generate the FE model due to the symmetry in structure. The SHELL element type is applied to deck, transverse, longitudinal bulkhead, girder, web frame and outer shell plating. Stiffeners and some heavy rigs are idealized with BEAM and MASS element–types, respectively. The same values of Young's modulus and Poisson's ratio in Table 1 are used in the ship hull structure as well. For some trivial parts that are not represented in FE model, their density is increased from increased from 7.85E+3 kg/m3 to 7.92E+3 kg/m3 to realize an actual ship weight. Numbers of elements and nodes in the FE model of ship hull structure are 8,717, and 3,959, respectively. The operation condition of the container ship is assumed to be the ballast condition. As shown in Figure 8(b), symmetric and asymmetrical boundary conditions are applied to the half breadth of ship hull structure to evaluate both ver-

tical and torsion-horizontal vibration modes. The wetted surface of ship hull structure is defined on the outer shell plating for the coupled analysis as represented in Figure 8(c), and the fluid density of sea water is 1.02E+3 kg/m3.

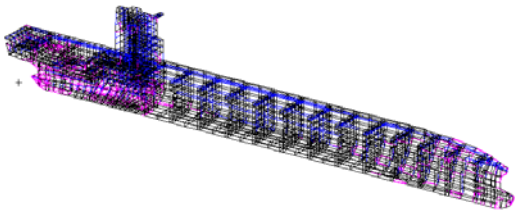

(a) Finite element model of ship hull structure

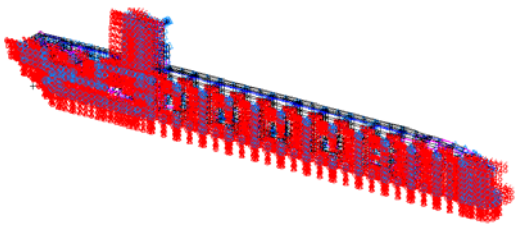

(b) Symmetric and asymmetrical boundary conditions

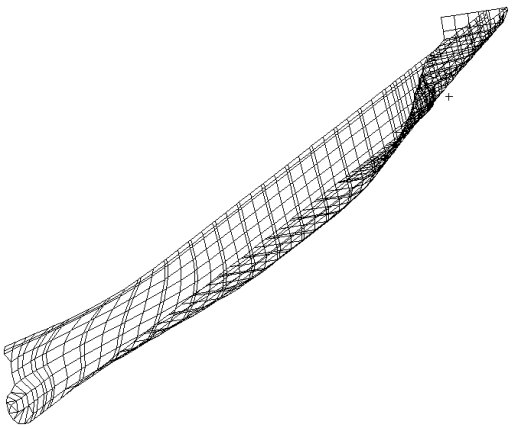

(c) Definition of interface in contact with fluid

Fig. 8. Ship hull structure for hydroelastic vibration analysis

The frequencies and mode results of vertical and torsion-horizontal vibration are represented in Table 7 and Figures 9(a) to 10(b), respectively. The comparisons of elastic and hydroelastic vibration results are also shown in Figure 11. As shown in Table 7, the lower first frequency results from torsion-horizontal vibration mode due to the structural characteristics of container ship. The frequency and mode results of hydroelastic vibration considering the fluid interface considerably differ from the elastic vibration in both vertical and torsion-horizontal vibration. The hydroelastic frequencies of ship hull structure is lower than the elastic due to the effect of added mass on the outer shell plating in contact with sea water. As shown in Figure 11, the fluid effect on the actual ship hull structure is increased in both vertical and torsion-horizontal vibration cases as each vibration mode is increased to the higher order.

Table 7. Vibration analysis results for ship hull structure [unit: Hz]

	Mode sequence	Elastic	Hydroelastic
Vertical vibration	1st	1.514	1.030
	2nd	3.121	2.094
	3rd	4.555	3.063
	4th	5.722	4.071
Torsion-horizontal vibration	1st	0.997	0.881
	2nd	2.948	2.555
	3rd	4.024	3.190
	4th	6.047	5.172

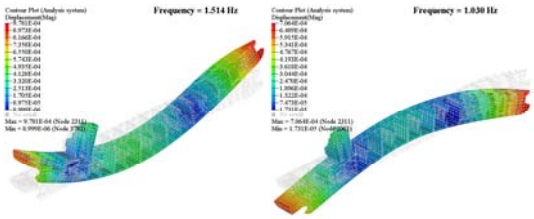

(i) 1st vertical vibration mode (left: elastic, right: hydroelastic)

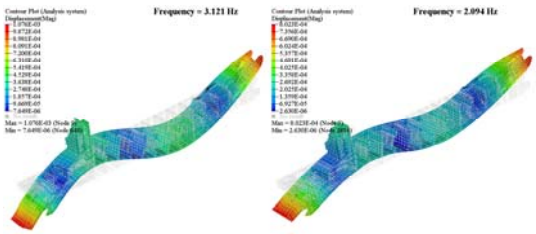

(ii) 2nd vertical vibration mode (left: elastic, right: hydroelastic)

Fig. 9(a). Vertical vibration results of ship hull structure (1st and 2nd modes)

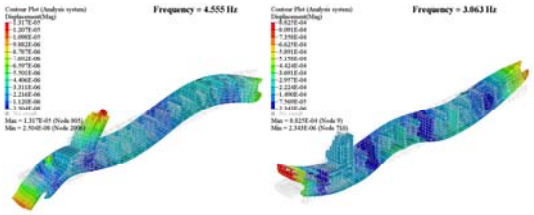

(i) 3rd vertical vibration mode (left: elastic, right: hydroelastic)

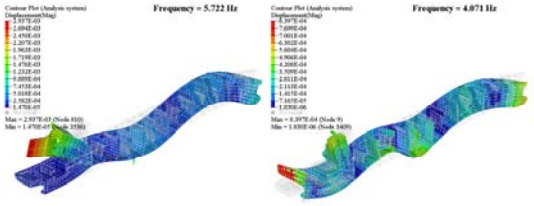

(ii) 4th vertical vibration mode (left: elastic, right: hydroelastic)

Fig. 9(b). Vertical vibration results of ship hull structure (3rd and 4th modes)

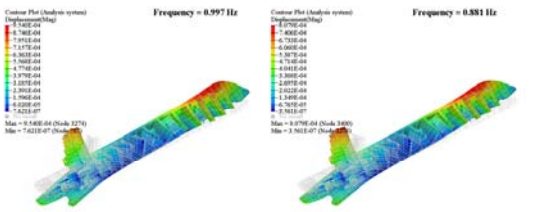

(i) 1st torsion-horizontal vibration mode (left: elastic, right: hydroelastic)

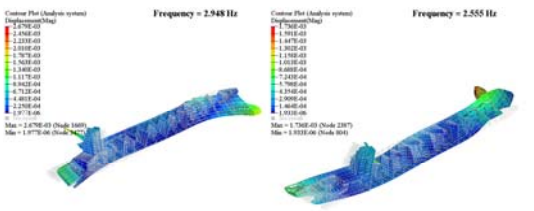

(ii) 2nd torsion-horizontal vibration mode (left: elastic, right: hydroelastic)

Fig. 10(a). Torsion-horizontal vibration results of ship hull structure (1st and 2nd modes)

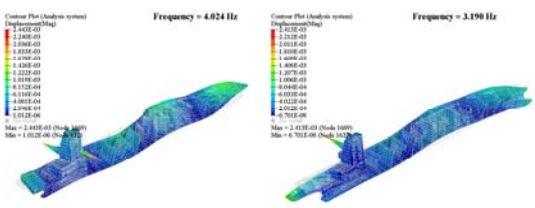

(i) 3rd torsion-horizontal vibration mode (left: elastic, right: hydroelastic)

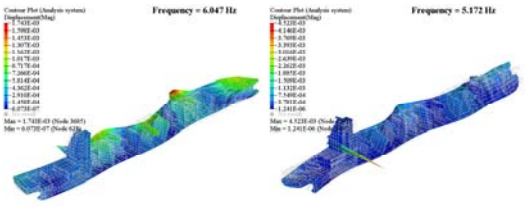

(ii) 4th torsion-horizontal vibration mode (left: elastic, right: hydroelastic)

Fig. 10(b). Torsion-horizontal vibration results of ship hull structure (3rd and 4th modes)

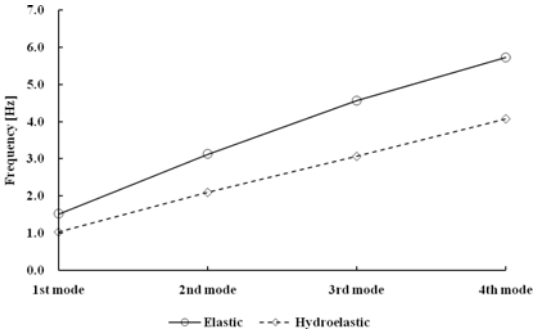

(a) Vertical vibration mode

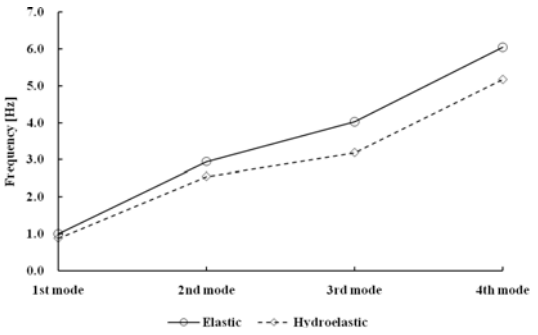

(b) Torsion-horizontal vibration mode

Fig. 11. Result comparison of ship hull structure vibration

The resonance with main excitation frequencies is also explored in the context of hydroelastic vibration modes as shown in Figure 12, wherein modal frequencies of ship hull structure have no possibility of resonance with main excitation sources under the operating range from NCR to MCR for both vertical and torsion-horizontal vibration modes. As presented in the results of practical application, the hydroelastic approach should be significantly considered in vibration evaluation of a structure operating in fluid such as ship and offshore structure.

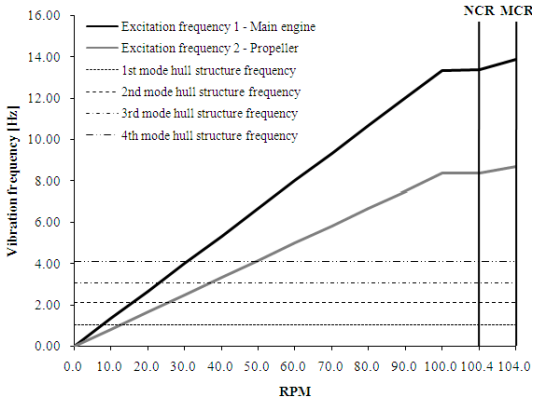

(a) Vertical vibration mode

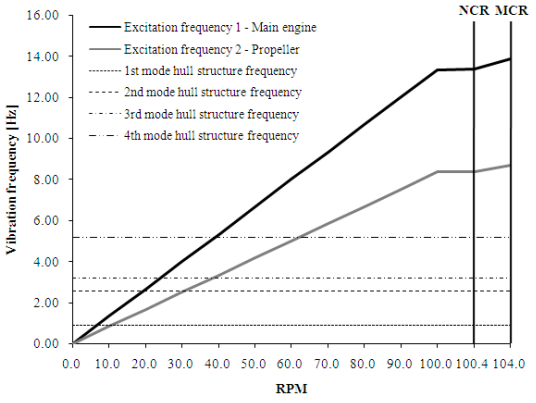

(b) Torsion-horizontal vibration mode

Fig. 12. Resonance curve for hydroelastic vibration of ship hull structure

5. Concluding Remarks

The present study discusses a finite element based coupled analysis to evaluate the vibration of structures in contact with fluid. Finite element analysis on various boundary conditions, vibration mode effect and submerged depth from free surface of the rectangular plate is carried out using the coupled analysis, and compared with the analytical solutions and experimental results. The hydroelastic vibration characteristics of the rectangular plate in contact with fluid are also compared with the elastic results in dry condition. The coupled analysis results of structure in contact with fluid tend to be more consistent with experimental results as the mode sequence is increased. The hydroelastic effect on the vibration of the rectangular plate is remarkably increased as the half of thickness is submerged in fluid. Once the plate is fully sunk in fluid, the variation of vibration characteristic is negligible up to an infinite submerged depth.

Subsequently, the hull structural vibration of 4,000 TEU container ship is considered for the practical application of coupled analysis. The hydroelastic vibration characteristics of ship hull structure contacted with sea water are evaluated on both vertical and torsion-horizontal vibration modes, and compared with the elastic results in dry condition. It is shown that the hydroelastic effect should be also considered for the vibration evaluation of structures in contact with fluid, and the coupled analysis plays an important role in such problems.

References

[1] O. C. Zienkiewicz and P. Bettes, *Fluid-Structure Dynamic Interaction and Wave Forces: an Introduction to Numerical Treatment*, Int J Numer Methods Eng, 13 (1978) 1–16.

[2] T. Kumai, *Added Mass Moment of Inertia Induced by Torsional Vibration of Ships*, Journal of Japan Society of Naval Architects and Ocean Engineers, 1(1) (1959) 93–100.

[3] L. Landweber and M. C. de Macagno, *Added Mass of Two–dimensional Forms Oscillating in a Free Surface*, Journal of Ship Research, 1(3) (1957) 20–9.

[4] R. L. Townsin, *Virtual Mass Reduction Factor J Values for Ship Vibration Calculations Derived from Tests with Beams Including Ellipsoids and Ship Models*, Trans RINA, 111(3) (1969) 385–97.

[5] C. A. Brebbia, J. C. F. Telles and L. C. Wrobel, *Boundary Element Techniques – Theory and Applications in Engineering*, Berlin, Springer-Verlag (1984).

[6] F. Axisa, *Modelling of Mechanical Systems, Vol. 3: Fluid–Structure Interaction*, Amsterdam, Elsevier (2006).

[7] H. J. P. Morand and R. Ohayon, *Fluid Structure Interaction*, New York, Wiley (1995).

[8] J. F. Sigrist and S. Garreau, *Dynamic Analysis of Fluid–structure Interaction Problems with Modal Methods using Pressure-based Fluid Finite Elements*, Finite Elements in Analysis and Design, 43(4) (2007) 287–300.

[9] K. T. Chung, *On the Vibration of the Floating Elastic Body using Boundary Integral Method in Combination with Finite Element Method*, Journal of the Society of Naval Architects of Korea, 24(4) (1987) 19–36.

[10]T. Chung, Y. B. Kim and H. S. Kang, *Hydroelastic Vibration Analysis of Structure in Contact with Fluid*, Journal of the Society of Naval Architects of Korea, 29(1) (1992) 18–28.

[11]B. Uğurlu and A. Ergin, *A Hydroelastic Investigation of Circular Cylindrical Shells-Containing Flowing Fluid with Different End Conditions*, J Sound Vib, 318(4–5) (2008) 1291–312.

[12]A. Ergin A and P. Temarel, *Free Vibration of a Partially Liquid-Filled and Submerged, Horizontal Cylindrical Shell*. J Sound Vib, 254(5) (2002) 951–65.

[13]S. H. Choi, K. S. Kim and S. W. Son, *Analytical and Experimental Study on Vibration Characteristics for Rectangular Tank Structure Filled with Fluid*, Journal of Korean Society for Noise and Vibration Engineering, 12(3) (2002) 195–203.

[14]Y. W. Kim and Y. S. Lee, *Coupled Vibration Analysis of Liquid-filled Rigid Cylindrical Storage Tank with an Annular Plate Cover*, J Sound Vib, 279(1–2) (2005) 217–35.

[15]K. H. Jeong and M. Amabili, *Bending Vibration of Perforated Beams in Contact with a Liquid*, J Sound Vib 298(1–2) (2006) 404–19.

[16]C. T. F. Ross, P. Köster, A. P. F. Little and G. Tewkesbury, *Vibration of a Thin-walled Prolate Dome under External Water Pressure*, Ocean Engineering, 34(3–4) (2007) 560–75.

[17]W. Wei, L. Junfeng and W. Tianshu, *Modal Analysis of Liquid Sloshing with Different Contact Line Boundary Conditions using FEM*, J Sound Vib, 317(3–5) (2008) 739–59.

[18]R. E. D. Bishop and W. G. Price, *Hydroelasticity of Ships*, Cambridge, Cambridge University Press (1979).

[19]W. G. Price and Y. Wu, *Hydroelasticity of Marine Structures*, London, Elsevier Science Publishers (1985).

[20]S. Aksu S and W. G. Price, K. R. Suhrbier and P. Temarel, *A Comparative Study of the Dynamic Behaviour of a Fast Patrol Boat Travelling in Rough Seas*, Marine Structures, 6(5–6) (1993) 421–41.

[21]W. G. Price, I. M. Salas and P. Temarel, *The Dynamic Behaviour of a Mono-hull in Oblique Waves using Two- and Three-dimensional Fluid Structure Interaction Models*, Trans RINA, 144 (2002) 1-26.

[22]S. E. Hirdaris, W. G. Price and P. Temarel, *Two- and Three-dimensional Hydroelastic Analysis of a Bulker in Waves*, Marine Structures, 16(8) (2003) 627–58.

[23]K. Iijima, T. Yao and T. Moan, *Structural Response of a Ship in Severe Seas Considering Global Hydroelastic Vibrations*, Marine structures, 21(4) (2008) 420–45.

[24]K. C. Kim, J. S. Kim and H. Y. Lee, *An Experimental Study on the Elastic Vibration of Plates in Contact with Water*, Journal of the Society of Naval Architects of Korea, 16(2) (1979) 1–7.

[25]MSC Software, *MSC.NASTRAN User's Manual Version 2008* (2008).

[26]S. S. Lee and M. C. Kim and D. R. Williamson, *Implementation of a Fluid-structure Interaction Formulation using MSC/NASTRAN*, MSC Aerospace Users' Conference, Newport Beach, California, #3597 (1997).

[27]M. Chargin and O. Gartmeier, *A Finite Element Procedure for Calculating Fluid-structure Interaction using MSC/NASTRAN*, NASA-TM-102857 (1990).

[28]R. N. Coppolino, *A Numerically Efficient Finite Element Hydroelastic Analysis, Volume I: Theory and Results*, NASA-CR-2662, (1976).

[29]R. D. Blevins, *Formulas for Natural Frequency and Mode Shape*, Florida, Krieger (1993).

[30]C. Y. Song, C. Y. Son and J. Y. Song, *Bending-torsion Vibration Characteristics of Large Structures Influenced by Coupling Effects*, Journal of Korean Society for Noise and Vibration Engineering, 6(4) (1996) 431–38.